

# PID Evaluation of Transparent Backsheet Modules

Julien Dupuis<sup>1</sup>[\[https://orcid.org/0000-0002-2051-3079\]](https://orcid.org/0000-0002-2051-3079), Romain Bodeux<sup>1,2</sup>[\[https://orcid.org/0000-0001-7182-5083\]](https://orcid.org/0000-0001-7182-5083),  
Christine Abdel-Nour<sup>1</sup>[\[https://orcid.org/0009-0003-6430-3297\]](https://orcid.org/0009-0003-6430-3297), Dominique Loisnard<sup>1</sup>, Julien Tremblay<sup>1</sup>,  
Paul Lefillastre<sup>3</sup>, and Axel Becker<sup>3</sup>

<sup>1</sup>Electricité de France, France

<sup>2</sup>Institut Photovoltaïque d'Île-de-France, France

<sup>3</sup>EDF Renouvelables, France

**Abstract.** This Work Deals with the Robustness of Transparent Backsheet Modules using Coating/PET/PVF (TPC) Polymer Layers when Exposed to an Extended Potential Induced Degradation (PID) Stress based on IEC 61215. Results show a Significant Power Decrease on the Front Side after 576h of Testing for Negative Voltage with Three Time more Impact at the Rear Side Despite the Absence of Glass. PID is Confirmed with Electroluminescence (EL) and Photoluminescence (PL). Measurements Showing the Appearance of Dark Areas on Several Cells and an Inhomogeneous Signal all Along the Module with "Light trails". Moreover, Transmission Electron Microscopy Measurement Points out Sodium Presence at Both Cell Interface Despite POE Encapsulant and the Absence of Glass at the Rear Side. Two Types of PID Seem to be Present: Low Light Current-Voltage Measurements Suggest the Presence of PID-Potential at the Rear Side of the Cells And the Dark Area Could Be linked To PID-Corrosion Effect as Depassivation is observed with EL and PL.

**Keywords:** Transparent Backsheet, Potential Induced Degradation, Photovoltaic Module

## 1. Introduction

The application of transparent backsheet is now a viable alternative to glass to build a bifacial module [1-5]. Its main advantages are the cost of this solution which is also usually lower than glass, a significant lower weight, a better transparency and the possibility to keep a heat strengthen glass at the front side to better protect the module to hail. Moreover, transparent backsheets could also reduce PID due to its absence of sodium which limits the risk of PID at the rear side of the cells. Thus, this paper aims at studying the robustness of modules built with a transparent backsheet when exposed to extended Potential Induced Degradation (PID) stress.

## 2. Experimental

### 2.1. Modules' properties

Modules used in this study are p-PERC glass-backsheet modules from a tier-one manufacturer. The main modules properties are listed in the Table 1.

**Table 1.** Modules' properties.

<b>Module power</b>	390 Wp
<b>Bifaciality</b>	70 %
<b>Front glass thickness</b>	3.2 mm
<b>Encapsulant</b>	POE/POE
<b>Rear backsheet type</b>	Coating/PET/PVF
<b>Rear backsheet thickness (µm)</b>	20/275/25

## 2.2. Testing protocol

Five modules are first preconditioned using current injection at  $I_{sc}$  during 486h at 75°C with current-voltage measurement control every 162h. We use this procedure to avoid any Light Induced Degradation (LID) or Light and elevated Temperature Induced Degradation (LeTID) during the PID test phase [6-7].

Then a PID testing is done based on IEC 61215 standard (MQT 21) at 85°C and 85% RH with an extended time up to 576h instead of the required 96h in the standard. Modules are tested in the chamber with several polarizations (IV monitoring every 96h or 192h) :

- 1 reference module (outside the chamber)
- Mod1: module polarized at 0 V
- Mod2: module polarized at +1500 V
- Mod3: module polarized at -1500 V
- Mod4: module polarized at -1500 V

Then sampling method was applied to the PV module. The samples include the complete cell, i.e. glass, encapsulant, cells with interconnects and backsheets. In this method, the cells of modules Mod3 are cut using a cutting wheel. Two full cell pieces were obtained called Mod3-1 and Mod3-2. Then, the cell Mod3-1 is cut into a small piece of 1 cm X 1 cm using a diamond wire saw. The cross section of the sample is polished using ionic polishing Arblade5000 Hitachi. Cross-sectional samples are obtained using an FEI Helios DualBeam Focus-Ion-Beam (FIB) miller. The samples are listed in Table 2.

**Table 2:** List of the samples cut from the module.

<b>Module</b>	<b>Cell cut using cutting wheel</b>	<b>Sample using diamond wire saw and ionic polishing</b>
Mod3	Mod3-1	Mod3-1-1
	Mod3-2	

## 2.3. Characterization's equipments

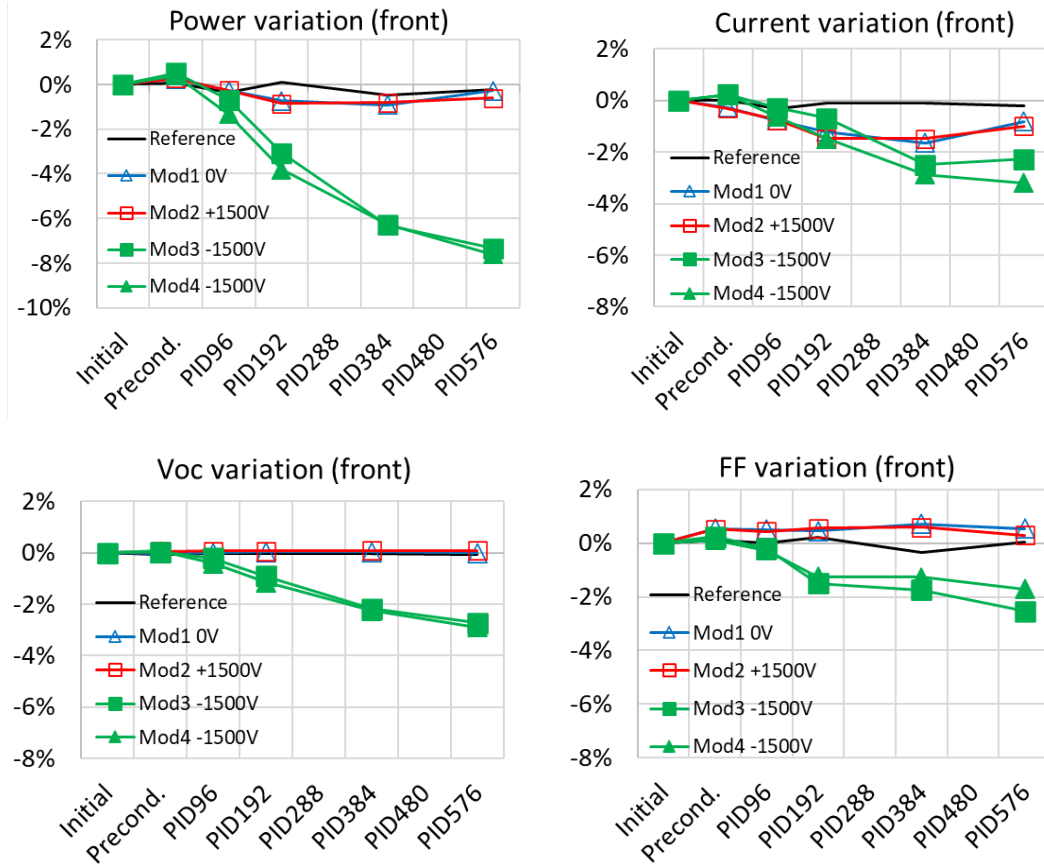
Electrical characterization of the PV modules was carried out using a PASAN flash tester Sun-Sim 3b with class AAA. Electroluminescence (EL) measurements were done by a Greteye Lumi Solar Professional system at the module level.

Encapsulated cells were then cut from the module in order to perform photoluminescence (PL) measurements using a BT Imaging LIS-R2 and lastly Transmission Electron Microscopy (TEM) carried out using an "Osiris" device from the manufacturer FEI. TEM acquisition was carried out using 200 keV energy.

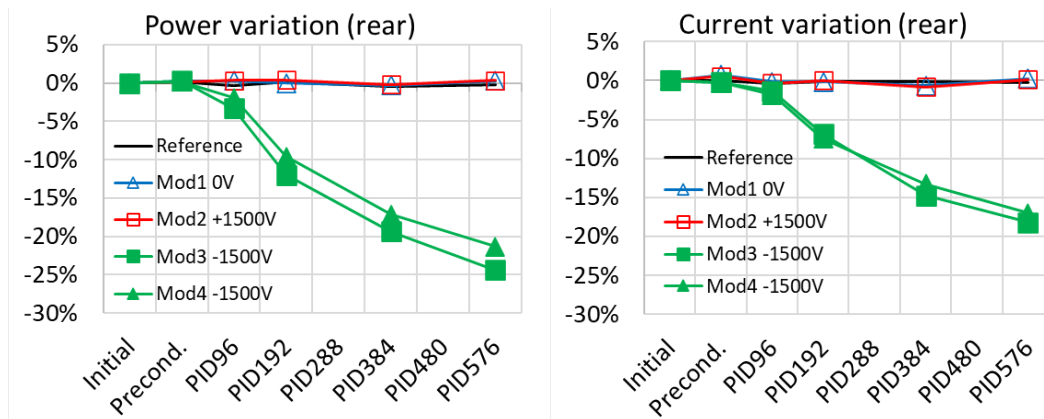
### 3. Results

#### 3.1. Current-voltage (I(V)) characterizations

The module's performance evolution with PID testing is plotted in the Figures 1 and 2 for the front and rear side respectively.



**Figure 1.** Front side module performance evolution during extended PID testing.



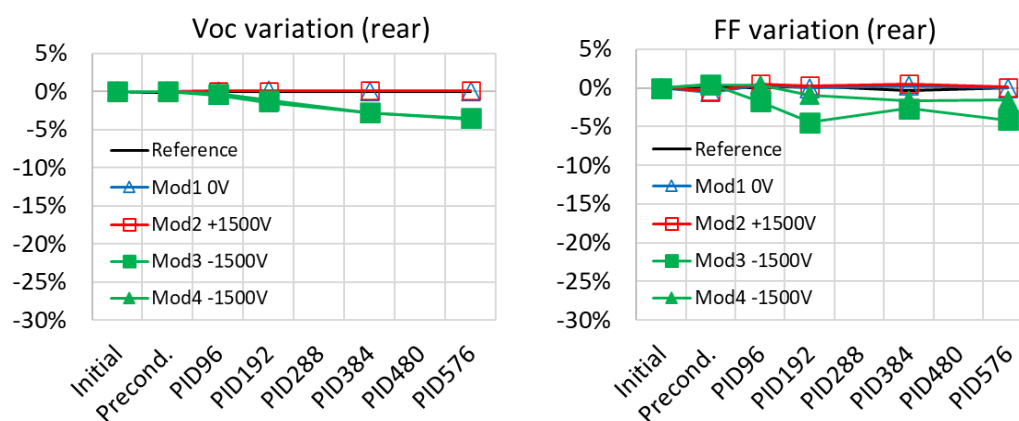


**Figure 2.** Rear side module performance evolution during extended PID testing.

Regarding the front side, the module's performance was not impacted by the positive or neutral voltages applied as shown in Figure 1. After the testing procedure, all electrical parameters measured for the tested modules were similar to those of the untested reference module. On the contrary, the application of negative voltage revealed a PID sensitivity with a power decrease up to almost 8% at the front side after the 576h of PID. Regarding the rear side, the performance degradation was three times more severe with a decrease of 25% and a large contribution of the current variation as shown in Figure 2.

### 3.2. Electroluminescence and photoluminescence characterization

To better understand the root cause of the performance degradation, EL and PL measurements were done on the "Mod3" and "Mod4" modules. EL picture of Mod3 and PL picture of Mod3-1 are presented in the Figure 3. Due to the PL measurements carried out on encapsulated cells cut out of the module, cell and glass cracks are visible on the pictures.

EL pictures show a general signal decrease after the testing as well as some punctual dark areas. Some "light trails" are also visible on most of the solar cells with locally higher EL intensity. These dark areas and trails are also confirmed by PL measurements pointing out a potential local passivation change.

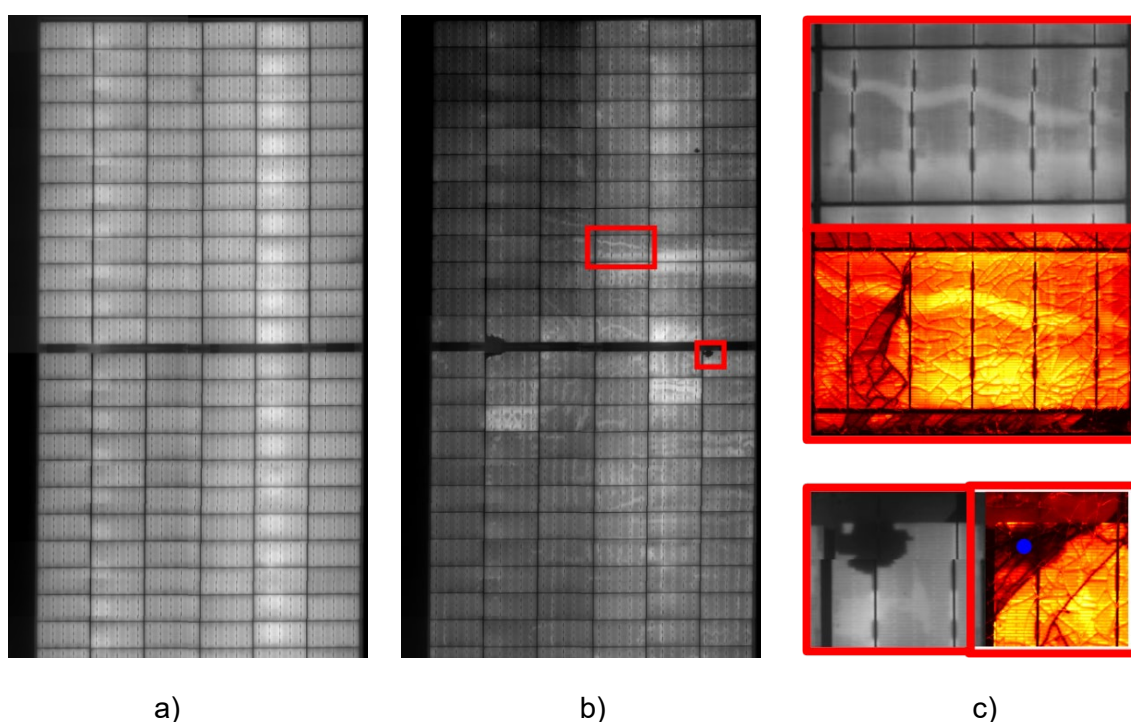


**Figure 3.** a) EL pictures of Mod3 at  $I_{sc}$  after preconditioning; b) after 576h of PID; c) Top: EL and PL pictures of a zoomed cell; bottom: EL and PL pictures of one of the dark area. The blue dot indicates the place where the TEM cross section analysis has been done.

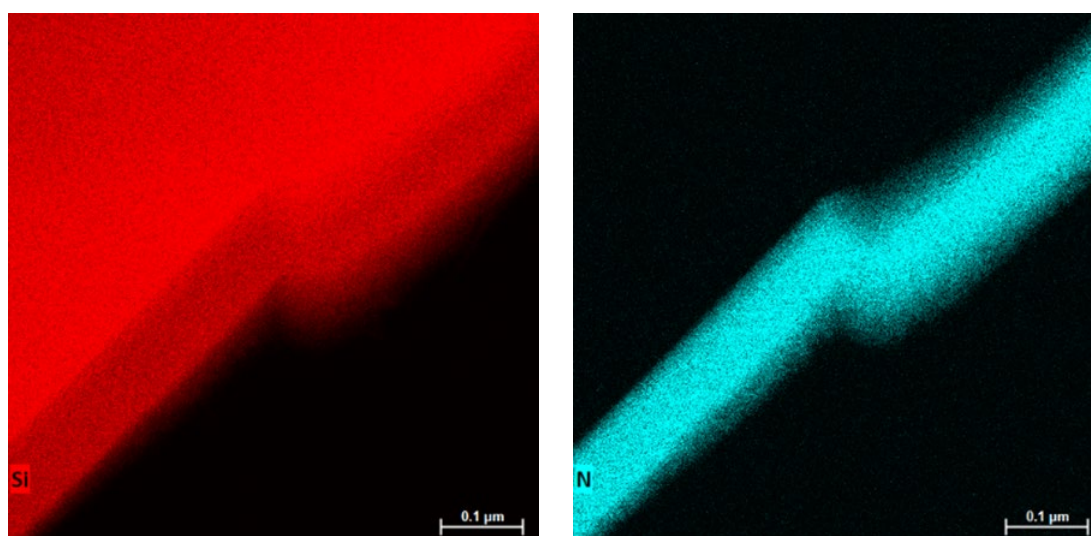
## 4. Discussion

Previous current-voltage, EL and PL measurements suggest the presence of two types of PID effect in the module: PID potential type (PID-p) and corrosion type (PID-c). The shunt type of PID-s, usually related to the migration of sodium ions coming from the glass to the cell, seems not to be present as no full shunted cells are visible and current voltage variation did not show any significant fill factor or  $V_{oc}$  decrease [8]. These ions can penetrate through the silicon and degrade the PN junction as demonstrated by [9]. PID-p on its side, can appear when the surface charge is modified because of ions migration or dielectric passivation fixed charge modification caused by the module polarization. Minority carrier become more attracted to the contacts and recombination is enhanced [10-11]. Low light current voltage measurement can give some indication on the presence of PID-p according to Luo et al. [10]. Lastly, PID-c was detected in bifacial solar cells by Sporleder et al. [12] and, for silicon PERC cells consisting in the rear passivation degradation based on cathodic corrosion phenomenon.

### 4.1. PID-c detection

In order to validate the PID-c hypothesis, study of the front and rear solar cell dielectric was carried out using TEM. Sampling method is used to remove the sample Mod3-1-1 from the dark area (blue dot area in Figure 3c). Elements mapping of the cross section of the front side of the silicon cell is presented in the Figure 4.

Although no structural modification of the front  $SiO_x/SiN_x/SiO_x$  and  $Al_2O_3/SiN_x$  passivation layers was found and despite the resistive POE encapsulant, the analysis performed highlights the presence of sodium particles at the front and rear surface of the solar cells. As no sodium was directly detected in the silicon itself, it is hard to be sure that sodium has merged through the passivation layers of the solar cells. Moreover, previous works on PID-s effect have emphasized the full darkening of the shunted cells during EL measurement which was not the case here even for lower current injection. Thus, even if sodium is present, this is suggesting that these dark areas are not linked to silicon PN junction shunt by the sodium ions. Thus, even if the dark area appearance is certainly linked to de-passivation effect as EL and PL image show the same dark area, no direct culprit was found.





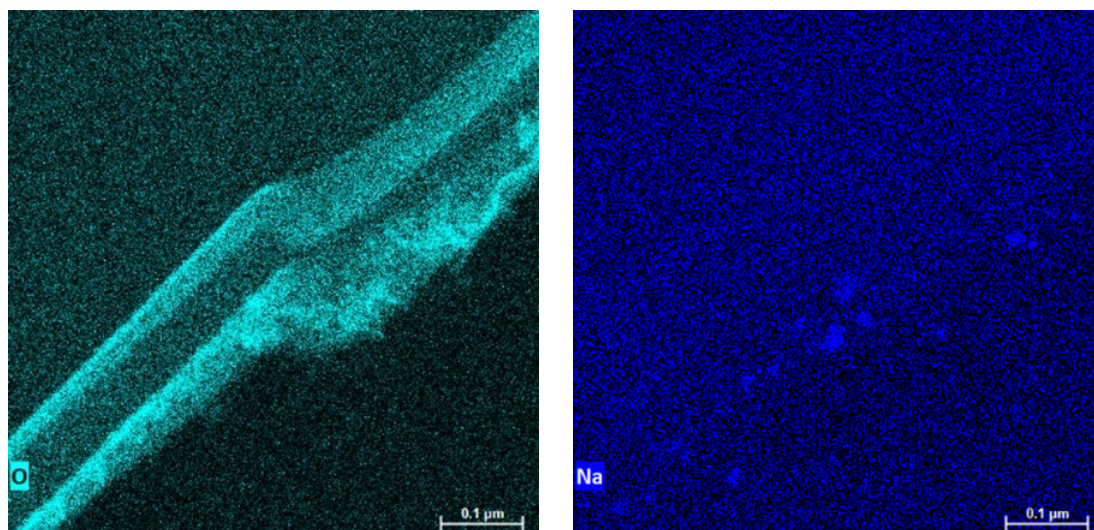
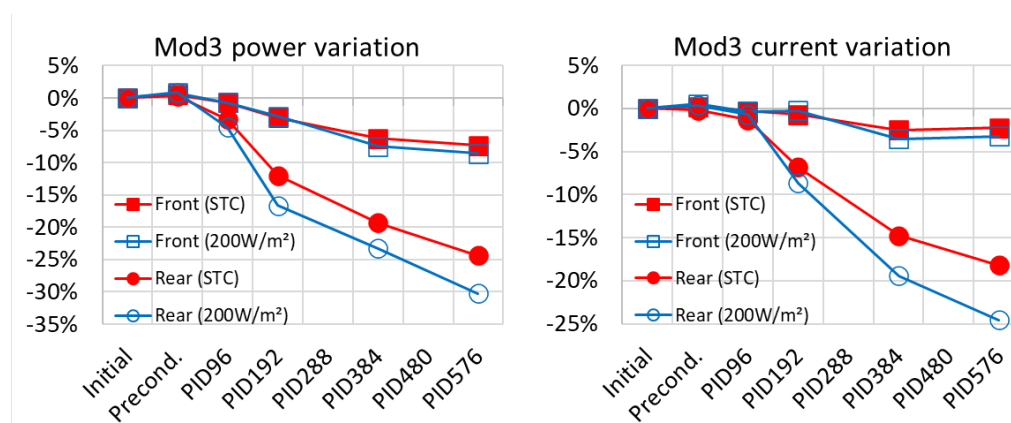


**Figure 4.** TEM's element detection at the silicon cell front interface (cross section Mod3-1-1).

## 4.2. PID-p detection

Low light I(V) measurements ( $200 \text{ W/m}^2$  irradiance) were plotted with STC measurements ( $1000 \text{ W/m}^2$ ) for the front and rear sides in Figure 5. STC and low light values found in this work give similar trend as observed by Luo et al. [10] in presence of PID-p with a high  $I_{sc}$  degradation and only slight FF decrease. The observed plateau reached by all the value in Luo and al. work is not reached in our case. This can be caused by the dark areas observed in our luminescence measurement that are extending with the increase of the PID testing time (not shown here) and thus increase the degradation.

PID-p effect is caused by charge accumulation at the rear side in the case of the PERC cells. Sodium presence near the passivation layer may be involved but as PID-p seems not requiring necessary charged ions to occur as discussed in [11], we can't conclude about its role.



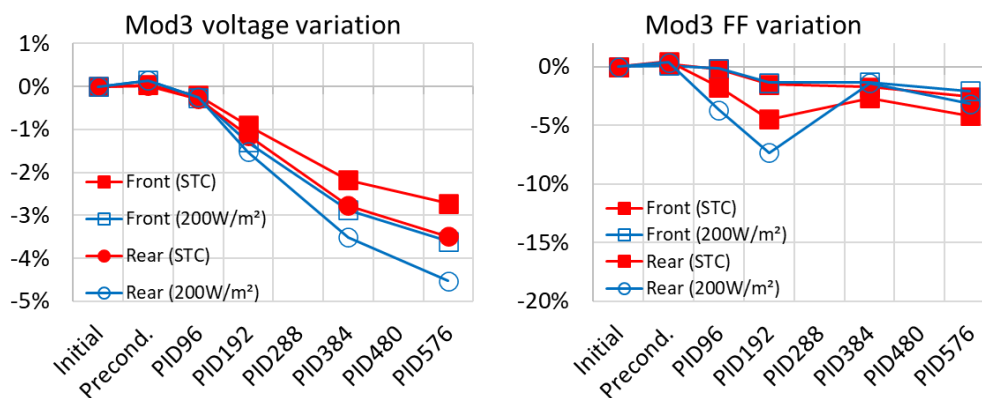


**Figure 5.** Comparison of low light and STC current voltage measurement of Mod3 module.

## 5. Conclusion

Bifacial modules with transparent backsheet were tested to extended PID stresses. I(V), EL and PL results highlighted two types of PID. Observed local cell depassivation could be linked to PID-c even if no direct evidence was observed using TEM measurement. PID-p is certainly present at the rear side of the samples as highlighted by the low light and STC I(V) results. Although its origin is not yet fully identified, the sodium in contact with the passivation layer can't be excluded as a degradation factor. The role of the transparent backsheet itself in the degradation is still unknown, more characterizations are in progress to detect possible degradation.

## Data availability statement

All relevant raw data were submitted with the article and can be asked directly to the authors.

## Author contributions

Julien Dupuis: Conceptualization, Investigation and Writing (original draft)

Romain Bodeux: Conceptualization, Investigation and Writing (review)

Christine Abdel-Nour: Formal Analysis and Writing (review)

Dominique Loinsard: Investigation and Formal analysis

Julien Tremblay: Investigation and Formal analysis

Paul Lefillastre: Resources and Supervision

Axel Becker: Supervision and Funding acquisition

## Competing interests

The authors declare no competing interests.

## Acknowledgement

The authors are very grateful to the EDF R&D laboratory team for the help provided in performing module testing.

## References

1. R. Kopecek and J. Libal, "Bifacial Photovoltaics 2021: Status, Opportunities and Challenges", *Energies* 2021, 14, 2076. <https://doi.org/10.3390/en14082076>
2. H. Park, S. Chang, S. Park and W. K. Kim, "Outdoor Performance Test of Bifacial n-Type Silicon PV modules", *Sustainability* 2019, 11, 6234, <https://doi.org/10.3390/su11226234>
3. W. Gambogi, M. Demko, B-L. Yu, S. Kurian, S. MacMaster, K. R. Choudhury, J. Tracy, D. Hu and H. Hu, "Transparent Backsheets for Bifacial Photovoltaic Modules", *Proceedings of the 47th IEEE Photovoltaic Specialists Conference*, pp. 1651-1657 Virtual meeting, 2020, <https://doi.org/10.1109/PVSC45281.2020.9300924>
4. W. Gambogi, M. Demko, T. Felder, S. MacMaster, B-L. Yu, A. Borne, H. Hu, Z. Pan and K. R. Choudhury, "Performance and reliability of bifacial modules using a transparent backsheet", *Proceedings of the 36th European Photovoltaic Solar Energy Conference and Exhibition*, pp. 1054-1058, Marseille, France, 2019, <https://doi.org/10.4229/EUPVSEC20192019-4AV.1.30>
5. C. Molto, J. Oh, F. I. Mahmood, M. Li, P. Hacke, F. Li, R. Smith, D. Colvin, M. Matam, C. DiRubio, G. Tamizhmani, H. Seigneur, "Review of Potential-Induced Degradation in Bifacial Photovoltaic Modules", *Energy Technol.* 2023, 2200943, <https://doi.org/10.1002/ente.202200943>
6. J. Dupuis, G. Plessis, G. El Hajje, E. Lajoie-Mazenc, E. Sandré, K. Radouane, P. Dupeyrat, "Light- and elevated temperature-induced degradation impact on bifacial modules using accelerated aging tests, electroluminescence, and photovoltaic plant modeling", *Prog Photovolt Res Appl.* 29 (2021) pp. 694–704, <https://doi.org/10.1002/pip.3345>
7. Z.Y. Yeo, Z.P. Ling, J.W. Ho, Q.X. Lim, Y.H. So and S. Wang, "Status review and future perspectives on mitigating light-induced degradation on silicon-based solar cells", *Renewable and Sustainable Energy Reviews* 159, pp. 112223, 2022, <https://doi.org/10.1016/j.rser.2022.112223>.
8. J. Carolus, J. A. Tsanakas, A. van der Heide, E. Voroshazi, W. De Ceuninck and M. Daenen, "Physics of potential-induced degradation in bifacial p-PERC solar cells", *Solar Energy Materials and Solar Cells* 200 (2019), 109950, <https://doi.org/10.1016/j.solmat.2019.109950>
9. V. Naumann, D. Lausch, A. Hähnel, J. Bauer, O. Breitenstein, A. Graff, M. Werner, S. Swatek, S. Großer, J. Bagdahn and C. Hagendorf, "Explanation of potential-induced degradation of the shunting type by Na decoration of stacking faults in Si solar cells", *Solar Energy Materials & Solar Cells* 120 (2014) pp. 383–389, <https://doi.org/10.1016/j.solmat.2013.06.015>
10. W. Luo, P. Hacke, K. Terwilliger, T. S. Liang, Y. Wang, S. Ramakrishna, A. G. Aberle, and Y. Sheng Khoo, "Elucidating Potential-induced Degradation in Bifacial PERC Silicon Photovoltaic Modules", *Prog Photovolt Res Appl.* 26 (2018) pp. 859–867, <https://doi.org/10.1002/pip.3028>
11. S. Yamaguchi, B. B. Van Aken, A. Masuda and K. Ohdaira, "Potential-Induced Degradation in High-Efficiency n-Type Crystalline-Silicon Photovoltaic Modules: A Literature Review", *Sol. RRL* 2021, 5, 2100708, <https://doi.org/10.1002/solr.202100708>
12. K. Sporleder, V. Naumann, J. Bauer, S. Richter, A. Hähnel, S. Großer, M. Turek, and C. Hagendorf, "Local Corrosion of Silicon as Root Cause for Potential-Induced Degradation", *Phys. Status Solidi RRL* 2019, 13, 1900163, <https://doi.org/10.1002/pssr.201900163>